Plant Cell Reports (2019) 38:59–74
https://doi.org/10.1007/s00299-018-2349-7

ORIGINAL ARTICLE

The Arabidopsis nucleoporin NUP1 is essential for megasporogenesis and early stages of pollen development

Shuguang Bao[1] · Guangshuang Shen[1] · Guichen Li[1] · Zhikang Liu[1] · Muhammad Arif[1] · Qingqing Wei[1] · Shuzhen Men[1]

Received: 18 August 2018 / Revised: 25 September 2018 / Accepted: 7 October 2018 / Published online: 19 October 2018

Abstract

Key message **Loss-of-function of nucleoporin NUP1 in Arabidopsis causes defect in both male and female gametogenesis. Its ovules are arrested during meiosis, and its pollen grains are aborted at mitosis I.**

Abstract Nuclear pore complex (NPC) plays crucial roles in nucleocytoplasmic trafficking of proteins and RNAs. The NPC contains approximately 30 different proteins termed nucleoporins (NUPs). So far, only a few of plant NUPs have been characterized. The Arabidopsis NUP1 was identified as an ortholog of the yeast NUP1 and animal NUP153. Loss-of-function of NUP1 in Arabidopsis caused fertility defect; however, the molecular mechanism of this defect remains unknown. Here, we found that both male and female gametogenesis of the *nup1* mutants were defective. *nup1* ovules were arrested from the meiosis stage onward; only approximately 6.7% and 3% ovules of the *nup1-1* and *nup1-4* mutants developed up to the FG7 stage, respectively. Pollen development of the *nup1* mutants was arrested during the first mitotic division. In addition, enlarged pollen grains with increased DNA content were observed in the *nup1* mutant. RNA-sequencing showed that expression levels of genes involved in pollen development or regulation of cell size were reduced dramatically in *nup1* compared with wild type. These results suggest that NUP1 plays an important role in gametogenesis.

Keywords Arabidopsis · Nuclear pore complex · Nucleoporin · NUP1 · Gametogenesis

Abbreviations

NPC	Nuclear pore complex
NUPs	Nucleoporins
NUP1	Nucleoporin 1
MMC	Megaspore mother cell
FG	Female gametophyte
FM	Functional megaspore
RNA-seq	RNA-sequencing

Communicated by Xian Sheng Zhan.

Electronic supplementary material The online version of this article (https://doi.org/10.1007/s00299-018-2349-7) contains supplementary material, which is available to authorized users.

✉ Shuzhen Men
shuzhenmen@nankai.edu.cn

[1] Department of Plant Biology and Ecology, College of Life Sciences, Nankai University and Tianjin Key Laboratory of Protein Science, Tianjin 300071, China

Introduction

The trafficking of RNAs and proteins between nucleus and cytoplasm is important for cellular function of eukaryotes (Xu and Meier 2008; Meier and Brkljacic 2009). The nuclear pore complex (NPC) plays crucial roles in these cellular activities. NPC is a nuclear envelope-embedded protein complex that is composed of approximately 30 nucleoporins (NUPs) (Walde and Kehlenbach 2010). The basic structure of NPC is conserved in vertebrates (Goldberg and Allen 1996), yeast (Allen and Douglas 1989) and plants (Roberts and Northcote 1970; Fiserova et al. 2009). Although NPC has been well characterized in vertebrates and yeast, the plant NPC is largely unclear.

A set of 26 NUPs were identified in Arabidopsis and rice by bioinformatics searches (Neumann et al. 2006). Then 30 Arabidopsis NUPs were identified using interactive proteomic approach (Tamura et al. 2010). So far only a few of plant NUPs have been characterized by physiological and genetic methods (Xu and Meier 2008; Meier and Brkljacic 2009; Yang et al. 2017). These studies demonstrated that plant NUPs were involved in diverse biological processes.

The Arabidopsis NUP96, NUP88, NUP160, SEH1, NUP98, CPR5, NUP82, and NUP1/NUP136 were reported to play important roles in disease resistance (Zhang and Li 2005; Cheng et al. 2009; Wiermer et al. 2012; Genenncher et al. 2016; Gu et al. 2016; Tamura et al. 2017). NUP160 was required for plant response to cold stress (Dong et al. 2006; Yang et al. 2017). NUP85, NUP160, and SEH1 were essential for cell-death control (Du et al. 2016). NUP96, NUP160, and NUP62 were shown to be involved in response to the plant hormone auxin (Parry et al. 2006; Boeglin et al. 2016).

The Arabidopsis NUP1 was initially identified as a putative ortholog of yeast NUP1 and vertebrate NUP153 by bioinformatics analysis (Neumann et al. 2006). Subsequently, it was verified to be a NPC component by yeast two-hybrid screen, proteomic approach, subcellular localization analysis, and mRNA export assay (Tamura et al. 2010; Lu et al. 2010). Functional analysis demonstrated that Arabidopsis NUP1 was necessary for exportation of nuclear mRNA and maintenance of nuclear morphology (Tamura et al. 2010; Lu et al. 2010; Tamura and Hara-Nishimura 2011). *nup1* mutant displayed multiple developmental defects, including early flowering, short siliques, and aborted pollen grains (Tamura et al. 2010; Lu et al. 2010). However, it is so far unclear at which stage *nup1* pollen development is arrested and whether female gametogenesis in *nup1* is affected. And the underlying molecular mechanisms of these defects remain to be solved.

In this study, we found that loss-of-function of NUP1 resulted in lethality in both male and female gametophyte development in Arabidopsis. *nup1* ovules were arrested during meiosis; its pollen grains were arrested during mitosis I. Tetrad analysis indicated that the defective pollen phenotype was resulted from a sporophytic defect. We also observed enlarged pollen grains in *nup1* mutant. DNA content was increased in *nup1* pollen grains. RNA-sequencing (RNA-seq) showed that transcript levels of genes involved in reproduction and regulation of cell size were reduced in *nup1* compared with the wild type (WT). Altogether our data indicate that NUP1 is required for gametogenesis in Arabidopsis.

Materials and methods

Plant materials and growth conditions

Arabidopsis thaliana ecotype Columbia (Col-0) was used in this study. Arabidopsis mutants including *nup1-1* (SALK_104728), *nup1-4* (GK_098G11), and *qrt1* (SAIL_1159_C11) were obtained from the Nottingham Arabidopsis Stock Centre (NASC) (http://arabidopsis.info/). Arabidopsis plants were cultured under long-day condition (16 h light/8 h dark) at 22 ± 1 °C. Seeds were surface-sterilized and incubated at 4 °C for 3 days before being sown on Murashige and Skoog (MS) medium (Duchefa Biochemie, Haarlem, The Netherlands) supplemented with 1% (w/v) sucrose (Sangon Biotech, Shanghai, China) and 0.8% (w/v) plant agar (Duchefa Biochemie, Haarlem, The Netherlands).

Vector construction and generation of transgenic plants

Pro*NUP1:GUS* was generated by introducing the *NUP1* promoter fragment (− 1229 bp upstream of ATG) into the pGEENII-0229-GUS vector between *Xho*I and *Sma*I restriction enzyme sites (Men et al. 2008). The Pro*NUP1:NUP1-EGFP* construct was generated through a two-step reaction. First, the *NUP1* promoter fragment was ligated into the pGEENII-0229-*EGFP* vector (Zhang et al. 2016) between *Xho*I and *Sma*I sites, then the *NUP1* coding sequence without the stop codon and added with a linker (GCGGCAGCC) was introduced into the above-obtained construct between *Sma*I and *Spe*I sites (Primer sequences are available in Supplementary Table S1). These constructs were transformed into *Agrobacterium tumefaciens* strain C58C1 (pMP90/pJIC Sa-Rep). Arabidopsis transgenic plants were generated using floral dip method (Clough and Bent 1998).

Male and female gametophyte observation

Pollen grains were collected from opening flowers and observed using an Olympus BX63 microscope. For female gametophyte observation, floral buds at different developmental stages were fixed in ethanol:acetic acid at 3:1 (v:v) for at least 4 h, and then cleared in chloral hydrate solution (67 g chloral hydrate, 8.3 mL glycerol, and 25 mL distilled water) for 4 days. Ovules were dissected out of the pistil and observed by differential interference contrast (DIC) microscopy.

GUS staining

For GUS staining, tissues were immersed in staining solution (0.5 mg/mL 5-bromo-4-chloro-3-indolyl-β-D-glucuronide in 50 mM sodium phosphate buffer pH 7.0, 0.5 mM potassium ferricyanide, 0.5 mM potassium ferrocyanide, and 0.1% Triton X-100) and incubated at 37 °C overnight. Before observation, the stained materials were cleared in chloral hydrate solution overnight.

Pollen grain staining

For observation of pollen nuclei, pollen grains from anthers at developmental stages of 7–13 were stained with 2 μg/mL of 4′,6-diamidino-2-phenylindole (DAPI) (Sigma-Aldrich,

Steinheim, Germany) for 20 min at room temperature. And then observe by fluorescence microscopy. For pollen viability assay, anthers at developmental stage 12 were dipped in the Alexander's solution as described (Alexander 1969; Johnson-Brousseau and McCormick 2004).

Callose deposition observation

Inflorescences of WT and *nup1* mutant were fixed in FAA solution for 24 h and stained in 0.1% aniline blue in 100 mM Tris (pH 8.5) for 10 h. Female gametophytes with staining were separated from pistil using dissecting needle, and then callose deposition during megasporogenesis was observed using an Olympus BX63 microscope.

Paraffin section

Arabidopsis floral buds at different developmental stages were fixed in formalin-acetic acid-alcohol (FAA) fixative (50% ethanol, 10% acetic acid, 5% formaldehyde) for 24 h at 4 °C. The samples were dehydrated through a series of ethanol (70, 80, 90, and 100%, 1 h each), cleared with the 1:1 mixture of xylene and ethanol for 30 min, and then cleared with xylene for 1 h. Then the samples were embedded in paraffin and sectioned at 8–10 μm using a microtome (Leica RM2125RTS, Leica, Germany) and stained with safranin and fast green. The sections were observed under an Olympus BX63 microscope.

Flow cytometry

For nuclei preparation, mature pollen grains from 13-stage flowers were extracted in 1 mL nuclei extraction buffer (Galbraith et al. 1983). The nuclei suspension was then filtered, and propidium iodide was added to the nuclei solution at the final concentration of 50 g/mL and stained at 4 °C for 20 min before flow cytometry testing. Approximately 20,000 stained

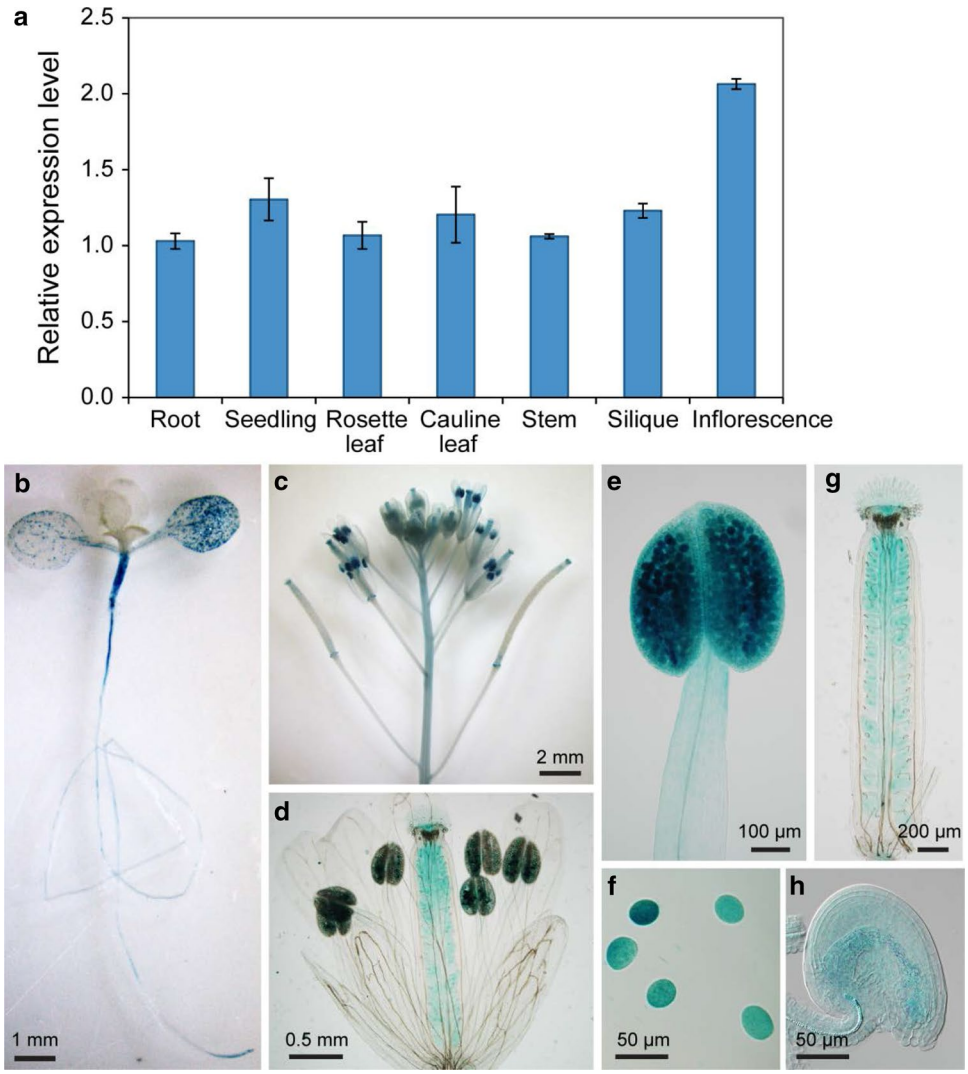

Fig. 1 Expression patterns of the Arabidopsis *NUP1* gene. **a** Analysis of *NUP1* expression levels by qRT-PCR. Expression levels relative to *ACTIN2* are displayed. The data represent the mean values ± SD of three experiments. **b**–**h** Expression of *ProNUP1:GUS* in various tissues, including 2-week-old plant (**b**), inflorescence (**c**), flower (**d**), stamen (**e**), pollen grains (**f**), pistil (**g**), and ovule (**h**)

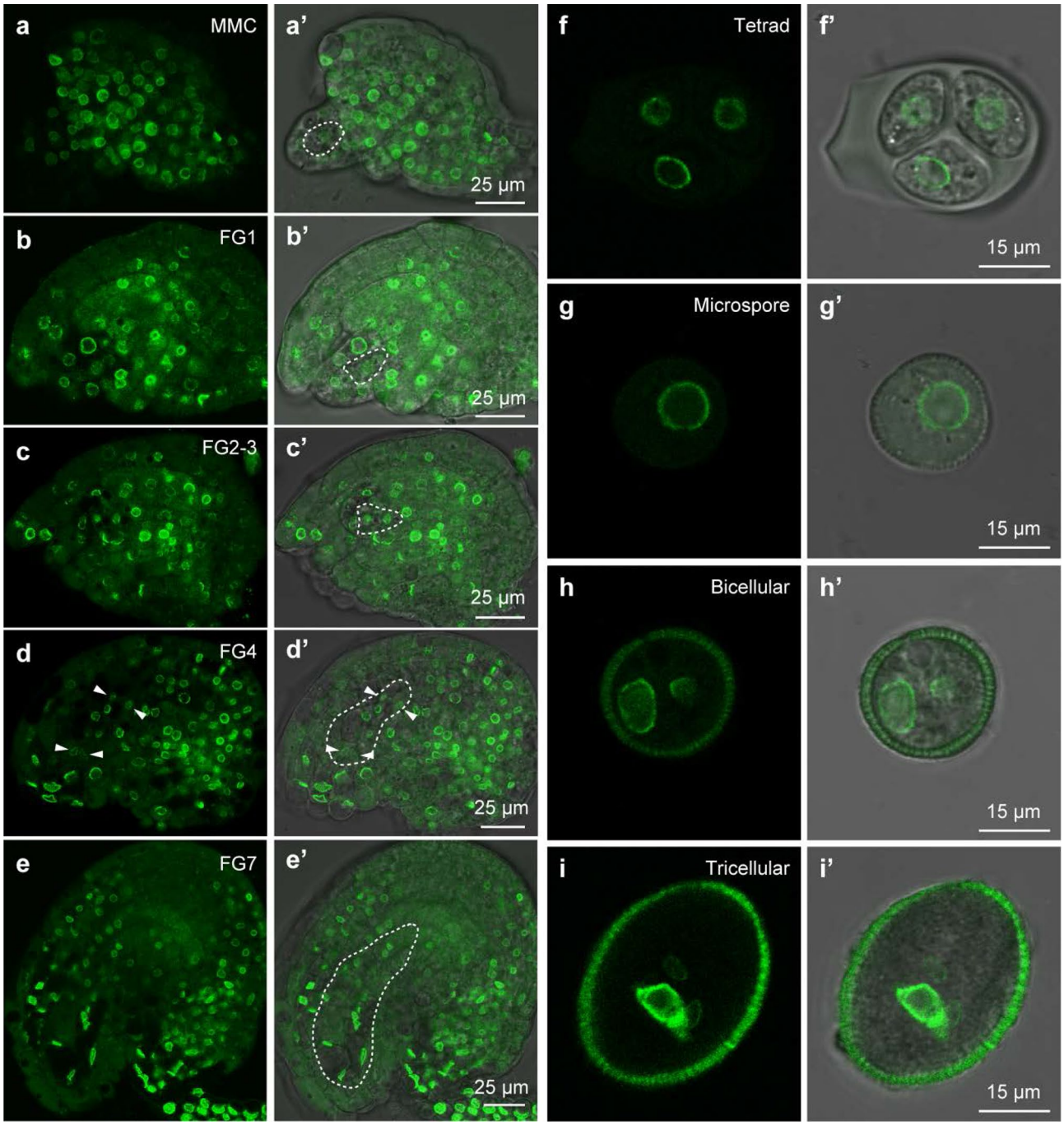

Fig. 2 NUP1 is expressed during ovule and pollen development. Ovules (**a**–**e**) and pollen grains (**f**–**i**) at various development stages of the *ProNUP1:NUP1-EGFP* transgenic plants were observed by confocal microscopy. White dotted lines encircle the embryo sac

nuclei were detected using flow cytometry equipment (FACS Calibur, BD).

Quantitative RT-PCR

For quantitative RT-PCR (qRT-PCR) analysis of *NUP1* expression pattern, total RNA was extracted from 7-day-old seedling, root, rosette leaf, cauline leaf, stem, inflorescence, and silique using Trizol reagent. For qRT-PCR verification of the expression levels of pollen development-related genes, total RNA was extracted from inflorescences containing stages 1–13 floral buds. The first-strand cDNA was prepared from 2 μg total RNA using EasyScript First-Strand cDNA Synthesis SuperMix kit (TransGen Biotech, Beijing, China).

qRT-PCR was performed using Eppendorf Realplex2 Detection System according to the manufacturer's protocol with qPCR SYBR Green Mixes (Takara, Dalian, China) in a final volume of 20 µL. Three technical repeats and three biological repeats were done for each reaction. Primer sequences are available in Supplementary Table S1.

RNA-seq and data analysis

Total RNA was extracted from inflorescences of WT and *nup1-4* plants using Trizol, and mRNA was enriched by oligo (dT) magnetic beads. The mRNA was fragmented into short fragments using fragmentation buffer and the first strand of cDNA was synthesized using random hexamer primers. Second-strand cDNA was synthesized by DNA polymerase I and RNase H. Then the cDNA libraries were constructed and sequenced using Illumina HiSeq2500 by Biomarker (Beijing, China). Clean reads were aligned to the Arabidopsis genome (TAIR10) using TopHat2 software (Kim et al. 2013). The Cuffdiff software was used to screen differentially expressed genes (Trapnell et al. 2012). Gene ontology (GO) analysis was performed using AgriGO (Du et al. 2010).

Results

NUP1 is highly expressed in male and female gametophytes

To investigate expression pattern of the Arabidopsis *NUP1* gene, qRT-PCR was performed. The results showed that the *NUP1* gene is expressed in most tissues examined, with the strongest expression level identified in inflorescence (Fig. 1a). To examine the *NUP1* expression in detail, the native *NUP1* promoter sequences (− 1229 bp upstream of ATG) were fused with the *GUS* reporter gene, and transformed into WT Arabidopsis. In 2-week-old *ProNUP1:GUS* transgenic plants, GUS staining was detected in hypocotyl, root tip and root vascular, and cotyledons (Fig. 1b; Supplementary Fig. S1). In cotyledons and hypocotyl, the GUS signal was not evenly distributed, some cells showed stronger GUS signal than other cells (Supplementary Fig. S1a-d). In root tip, the root cap cells showed stronger GUS signal than cells in the meristem and elongation zone (Supplementary Fig. S1f). In the inflorescence, the strongest GUS signal was detected in the anthers of opening flower (Fig. 1c). Detailed examination showed that GUS signal was mainly detected in pollen grains and ovules (Fig. 1d–h). *ProNUP1:GUS* was expressed throughout pollen and ovule development (Supplementary Fig. S2a–d), and its expression was highest in mature pollen grains (Supplementary Fig. S2c).

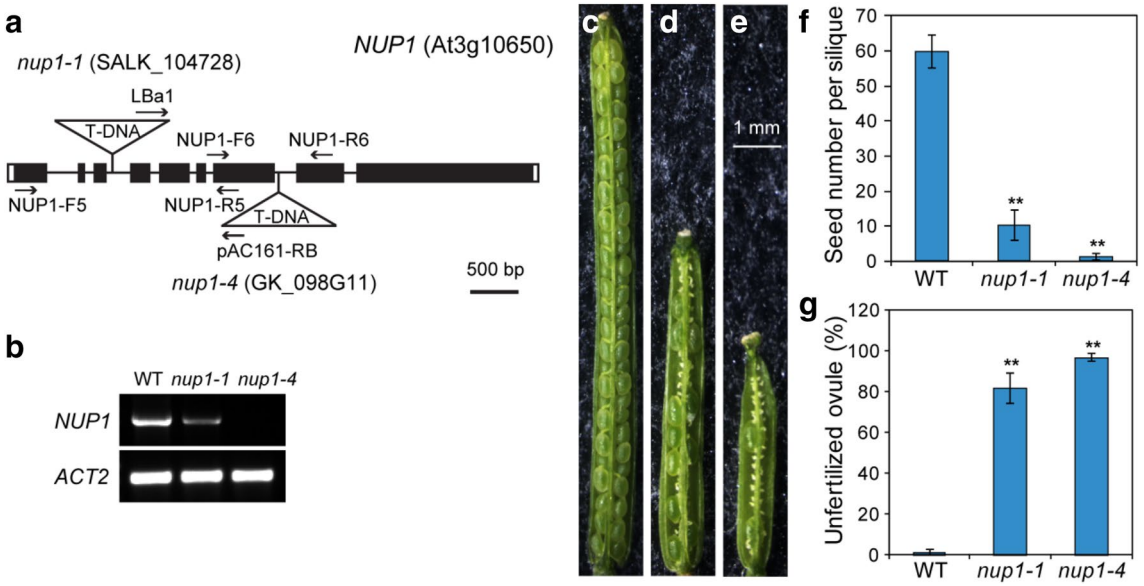

Fig. 3 Defective seed set in *nup1* mutants. **a** Schematic of T-DNA insertion sites in the *NUP1* gene. Black boxes indicate exons; white boxes indicate 5′ and 3′ untranslated regions; black lines indicate introns; triangles indicate T-DNA insertion sites; Arrows indicate the positions of primers. **b** RT-PCR analysis of the expression levels of the *NUP1* gene. The *ACTIN2* (*ACT2*) gene was used as an internal control. Total RNA was extracted from inflorescence. **c**–**e** Siliques 7–10 days post pollination from WT (**c**), *nup1-1* (**d**) and *nup1-4* (**e**) plants. Figures (**c**-**e**) share the same scale bar as shown in (**e**). **f, g** Quantification of total seeds and unfertilized ovules in siliques from WT, *nup1-1* and *nup1-4* plants. The data represent mean values ± SD ($n = 36$ siliques). $^{**}P < 0.01$ by Student's *t* test

Table 1 Analysis of mature siliques obtained from reciprocal crosses

Parental genotype (female × male)	Total seed number per silique (means ± SD)[a]	Unfertilized ovule (%) (means ± SD)
Col-0 × Col-0	51.2 ± 6.3	13.2 ± 5.4
Col-0 × *nup1-1*	23.3 ± 14.6	60.4 ± 18.7
nup1-1 × Col-0	9.2 ± 3.7	81.5 ± 7.2
nup1-1 × *nup1-1*	8.3 ± 1.9	83.4 ± 5.4
Col-0 × *nup1-4*	23.4 ± 15.2	61.6 ± 25.5
nup1-4 × Col-0	1.2 ± 1	97.6 ± 2.0
nup1-4 × *nup1-4*	1.0 ± 0.6	97.9 ± 1.4

[a] $n = 6$ to 7 siliques

To investigate subcellular localization of NUP1, we analyzed expression of a C-terminal EGFP-tagged NUP1 fusion protein in root, which was under control of the native NUP1 promoter (*ProNUP1:NUP1-EGFP*). The results showed that NUP1 is localized to nuclear envelope (Supplementary Fig. S3). We then analyzed *ProNUP1:NUP1-EGFP* expression during ovule and pollen development. NUP1-EGFP was expressed in all ovule cells throughout the ovule development (Fig. 2a–e). And GFP signal was also detected throughout the pollen development (Fig. 2f–i). In bicellular pollen, NUP1-EGFP was equally distributed in vegetative and generative nuclei (Fig. 2h), whereas in mature pollen grains, NUP1-EGFP signal was stronger in the vegetative nuclear envelope than in the sperm nuclei envelope (Fig. 2i).

Together, these results suggest that *NUP1* plays a role in male and female gametophyte development.

Deficiency of NUP1 affects both male and female gametophyte development

To study the potential role of Arabidopsis NUP1 in gametogenesis, we isolated two T-DNA insertion mutant alleles, *nup1-1* (SALK_104728) and *nup1-4* (GK_098G11) (Fig. 3a). *nup1-1* has been reported previously (Tamura et al. 2010; Lu et al. 2010), whereas *nup1-4* is a new mutant allele of the *NUP1* gene. RT-PCR analysis revealed that residual *NUP1* transcripts were present in the *nup1-1* mutant, whereas no *NUP1* transcripts were detected in the *nup1-4* mutant (Fig. 3b). Therefore, the *nup1-1* allele is a knock down mutant, whereas the *nup1-4* allele is a knock out mutant. Both *nup1-1* and *nup1-4* exhibit early flowering and short siliques phenotypes, and the siliques of *nup1-4* were shorter than that of *nup1-1* (Supplementary Fig. S4). Short undeveloped siliques suggest fertility defect. Therefore, we examined seed set in the *nup1* siliques. There were approximately 60 seeds per WT silique (Fig. 3c, f). However, in *nup1-1* and *nup1-4* siliques there were only approximately 10 and 1 seeds, respectively (Fig. 3d–f). In addition, siliques from *nup1-1* and *nup1-4* were found to have approximately 82% and 97% unfertilized ovules, respectively, compared with < 2% in WT (Fig. 3c–e, g). These results suggest that gametogenesis is affected in the *nup1* mutant. To verify this, we performed reciprocal crosses between *nup1* mutants and WT. When *nup1-1* or *nup1-4* pollen grains were used to fertilize WT ovaries, more than 60% of ovaries were not fertilized (60.4 ± 18.7 for *nup1-1*, 61.6 ± 25.5 for *nup1-4*) (Table 1). Similarly, when WT pollen grains were used to pollinate *nup1-1* or *nup1-4* ovaries, more than 80% of ovaries were not fertilized (81.5 ± 7.2 for *nup1-1*, 97.6 ± 2.0 for *nup1-4*) (Table 1). Together, these data demonstrate that both male and female gametes of *nup1* plants are defective.

To confirm that these fertility defects were caused by NUP1 loss-of-function, we introduced the *ProNUP1:NUP1-EGFP* into the *nup1-4* mutant. The transgene rescued all of the defects of the *nup1-4* mutant (Supplementary Fig. S5).

Fig. 4 *nup1* embryo sac phenotypes at maturity. **a** Diagram of female gametophyte development. Black dots indicate nuclei, grey ovals indicate vacuole. *MMC* megaspore mother cell, *Nu* nucellus, *FM* functional megaspore, *DM* degenerated megaspore, *V* vacuole, *AC* antipodal cell, *PN* polar nuclei, *EC* egg cell, *SC* synergid cell. **b–m** Differential interference contrast (DIC) images of embryo sacs dissected from WT (**b**) and *nup1-1* (**c–m**) flowers at developmental stage of 13. **b** WT female gametophyte at stage FG7. **c** Degenerated *nup1-1* female gametophyte. **d–l** Arrested *nup1-1* female gametophytes at stages of MMC (**d, e**), meiosis I (**f**), tetrad (**g** and **h; h** is a high-magnification image of **g**), FG1 (**i**) and FG2 (**j**). **k, l** delayed *nup1-1* female gametophytes at stages of FG4 (**k**) and FG6 (**l**). **m** *nup1-1* female gametophyte at stage FG7. *CN* central cell nucleus, *EN* egg cell nucleus, *SN* synergid cell nuclei, *N* nucleus, *DN* degenerating nucleus, *CW* cell wall, *DM* degenerating megaspore, *PN* polar nuclei, *AN* antipodal cell nuclei, *DES* degenerated embryo sac. Figures (**b–g, i–m**) share the same scale bar as shown in **m**

nup1 female gametophyte is arrested during meiosis

Because reciprocal crosses indicated that *nup1* mutants had defects in both male and female gametogenesis, we first analyzed the final phenotype of its female gametophyte (FG) by whole-mount clearing of ovules at mature stage. In Arabidopsis, megaspore mother cell (MMC) undergoes meiosis, resulting in four megaspores. Subsequently, three megaspores degenerate, leaving one functional megaspore (FM). Then the FM undergoes three rounds of mitosis without cytokinesis. After cellularization and polar nuclei fusion, the FM becomes a seven-celled female gametophyte, containing an egg cell, two synergids, a central cell, and three antipodals, which undergo cell death before fertilization (Fig. 4a). At maturity, approximately 97.7% of WT gametophytes reached FG7 stage ($n = 305$) (Fig. 4b; Table 2). By contrast, at maturity, 52.5% of the *nup1-1* ovules and 80% of the *nup1-4* ovules were collapsed and degenerated (Fig. 4c; Table 2); 10.2% of *nup1-1* ovules and 3.9% of *nup1-4* ovules were arrested either before or during the meiosis stage, as

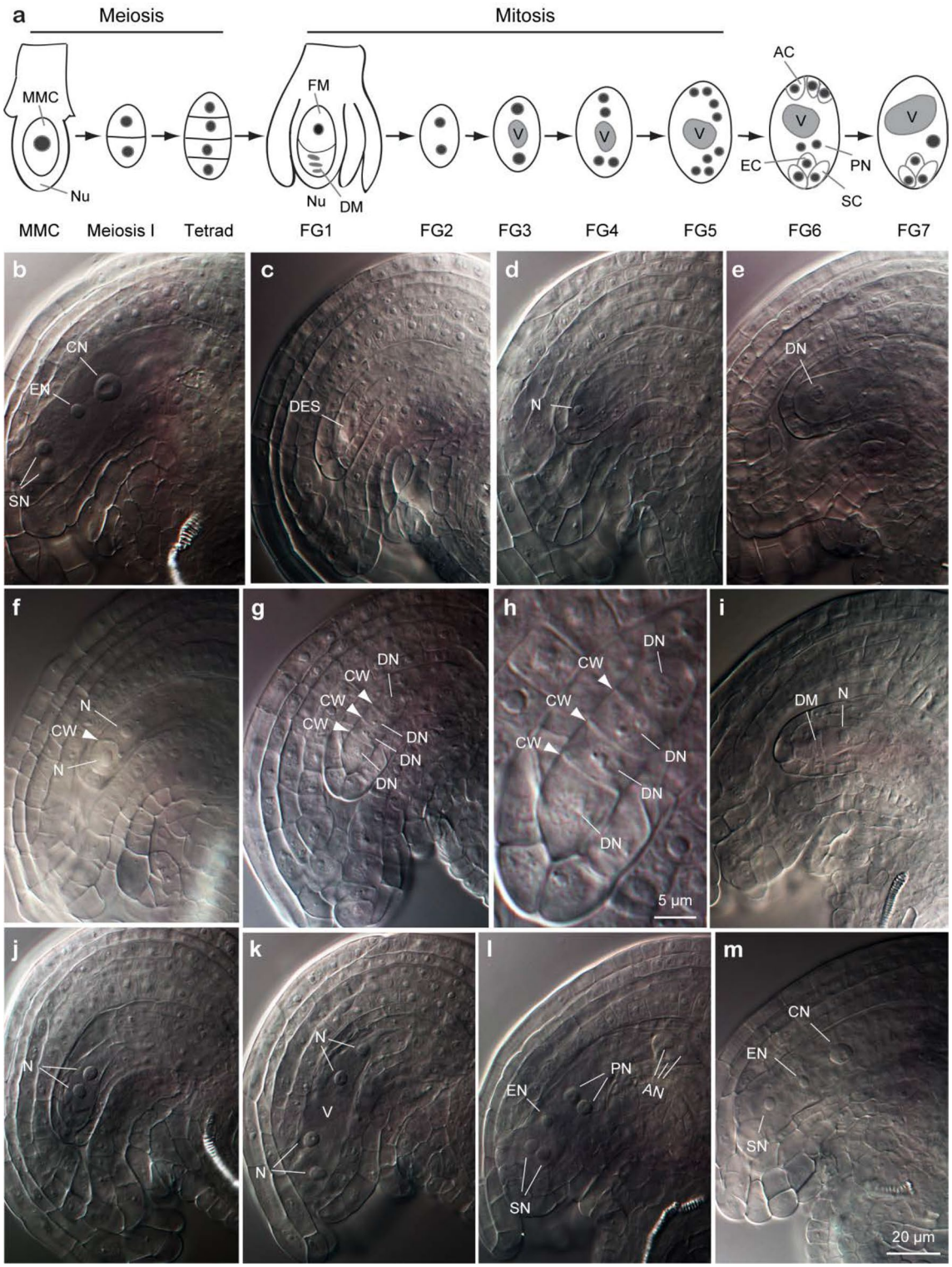

some ovules contained a MMC (Fig. 4d, e), some ovules contained a meiocyte in a dyad (Fig. 4f) and some ovules contained a tetrad (Fig. 4g, h); 15.9% of *nup1-1* ovules and 8.2% of *nup1-4* ovules were arrested at FG1 stage (Fig. 4i); 7.5% of *nup1-1* ovules and 2.4% of *nup1-4* ovules were arrested at FG2-3 stage (Fig. 4j); 3.6% of *nup1-1* ovules and 0.9% of *nup1-4* ovules were developed to FG4 stage (Fig. 4k); 3.6% of *nup1-1* ovules and 1.5% of *nup1-4* ovules reached FG5-6 stage (Fig. 4l); only 6.7% of *nup1-1* ovules

and 3.0% of *nup1-4* ovules reached FG7 stage ($n = 668$ for *nup1-1*, 330 for *nup1-4*) (Fig. 4m; Table 2).

To determine when the collapsed and degenerated *nup1* ovules were arrested, we analyzed WT and *nup1* ovules at various stages of development. In WT, female gametogenesis proceeds normally from MMC to FG7 (Supplementary Fig. S6), and is fairly synchronous within a pistil, spanning at most three neighboring developmental stages (Table 3). However, the developmental synchronicity was already impaired in the *nup1* pistils at the transition from MMC to FG1 stage, approximately 45% of *nup1-1* ovules ($n = 171$) and 78.2% of *nup1-4* ovules ($n = 202$) were degenerated before FG1 stage (Supplementary Fig. S6; Table 3). Taken together, these results indicate that most of *nup1* ovules were arrested either before or during the process of meiosis.

To further determine whether meiosis of ovules was affected in *nup1* mutant, we investigated the callose deposition which is a cytological marker for positioning of newly formed cell plate during first and second division of meiosis. In WT ovules, callose signal showed a bright band at

Fig. 5 Callose depositions during megasporogenesis are defective in *nup1* mutant. **a**–**h** Callose depositions during megasporogenesis in WT. **i**–**p** Abnormal callose depositions during megasporogenesis in *nup1-4* mutant. **q** Quantification of callose deposition at various stages of meiosis in 2-IV stage ovules in WT ($n = 46$) and *nup1-4* ($n = 114$). Figures (**a**–**p**) share the same scale bar as shown in (**p**)

Table 2 Phenotypic classes of female gametophytes dissected from stage 13 flowers

Genotype	FG0 (%)[a]	FG1 (%)	FG2–3 (%)	FG4 (%)	FG 5–6 (%)	FG7 (%)	Degenerated (%)	*n*
WT	0	0	0	0.3	1.3	97.7	0.7	305
nup1-1	10.2	15.9	7.5	3.6	3.6	6.7	52.5	668
nup1-4	3.9	8.2	2.4	0.9	1.5	3.0	80.0	330

[a]FG stages were defined as in Fig. 4a

Table 3 Synchrony of female gametophyte development in WT, *nup1-1*, and *nup1-4* plants

Pistil stage[a]	Percentage of female gametophytes at developmental stage (%)[b]							
	MMC	FG1	FG2–3	FG4	FG5–6	FG7	Degenerated	*n*
WT								
pil1	100							73
pil2	8.6	91.4						58
pil3		23.4	62.5	14.1				64
pil4			18.2	78.2	1.8		1.8	55
pil5				23	39.2	37.8		74
pil6					1.3	98.7		75
nup1-1								
pil1	100							165
pil2	20.5	34.5					45	171
pil3	15.5	28.9	14.2	1.7			39.7	232
pil4	13.7	27.4	12.3	8.2	1.4		37	73
pil5	11.4	22.8	6.3	7.6	6.3	3.8	41.8	79
pil6	12.8	15.2	4.8	1.6	2.4	16.8	46.4	125
nup1-4								
pil1	100							123
pil2	7.4	14.4					78.2	202
pil3	4.2	13.2	4.2				78.3	212
pil4	5.1	10.9	1.9	2.6			79.5	156
pil5	5.2	8.7	2.6	2.6	2.6		78.3	115
pil6	3.8	7.1	3.8	0.5	0.9	4.7	79.2	212

[a]Pistil developmental stages were assigned according to the dominant female gametophyte stage within a pistil. For example, in pil1, pil2, and pil3 most female gametophytes were at the stages of MMC, FG1, and FG2–3, respectively

[b]FG stages were defined as in Fig. 4a

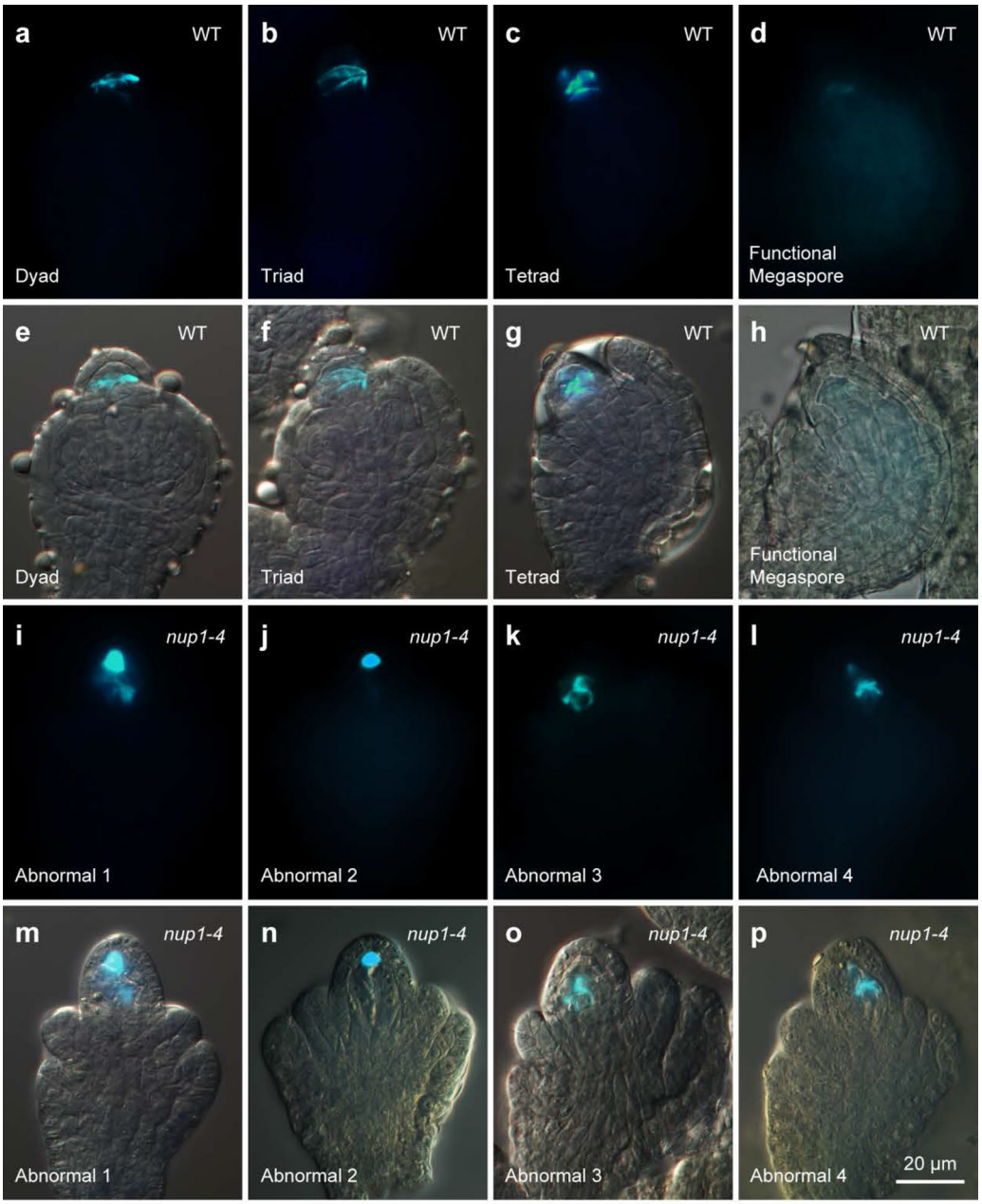
a WT
Dyad
b WT
Triad
c WT
Tetrad
d WT
Functional Megaspore
e WT
Dyad
f WT
Triad
g WT
Tetrad
h WT
Functional Megaspore
i nup1-4
Abnormal 1
j nup1-4
Abnormal 2
k nup1-4
Abnormal 3
l nup1-4
Abnormal 4
m nup1-4
Abnormal 1
n nup1-4
Abnormal 2
o nup1-4
Abnormal 3
p nup1-4
Abnormal 4
20 μm

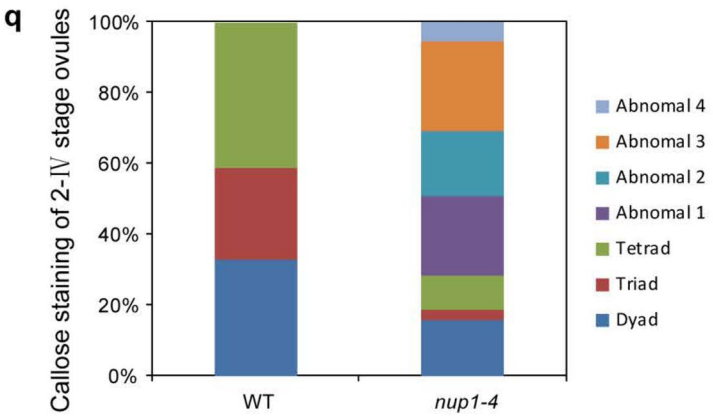
q
Callose staining of 2-Ⅳ stage ovules
100%
80%
60%
40%
20%
0%
WT
nup1-4
Abnomal 4
Abnomal 3
Abnomal 2
Abnomal 1
Tetrad
Triad
Dyad

the newly formed cell plates after the first meiotic division, called dyad (Fig. 5a, e). Then two bright bands of callose signal were observed at the early stage of second meiotic divison, called triad (Fig. 5b, f). After that, two bright bands and partial accumulation at the micropylar end of callose signal were observed after the second meiotic division, called tetrad (Fig. 5c, g). The callose signal almost disappeared after functional megaspore formation (Fig. 5d, h). In *nup1* ovules, the callose deposition showed dramatically abnormal distribution compared with WT, including the callose signal mainly focused at the micropylar end, named abnormal 1 (22.8%, $n = 114$) (Fig. 5i, m, q); all of the callose signal focused at the micropylar end, named abnormal 2 (18.4%, $n = 114$) (Fig. 5j, n, q); callose signal distributed pell-mell in embryo sac and no signal distributed at the micropylar end, named abnormal 3 (25.4%, $n = 114$) (Fig. 5k, o, q); and callose signal distributed on one side of embryo sac, named abnormal 4 (5.3%, $n = 114$) (Fig. 5l, p, q). The percentages of ovules at the dyad, triad, and tetrad stage of *nup1-4* were obviously reduced compared with WT (Fig. 5q). These results suggest that formed position of cell plate was affected during first and second meiotic division of *nup1* ovules.

Sporophytic mutation results in abortive pollen grains in *nup1* mutant

We next examined pollen development in *nup1* mutant. Alexander staining showed that the number of viable pollen grains in *nup1* anthers was significantly reduced compared with that of the WT (Supplementary Fig. S7). Approximately 53.5% of *nup1-1* pollen grains ($n = 1206$) and 59.3% of *nup1-4* pollen grains ($n = 1163$) were shriveled (Supplementary Fig. S7e, f). By contrast, less than 0.5% of the pollen was shriveled in WT anthers ($n = 1118$). We further examined the pollen morphology by scanning electron microscopy. Pollen grains from WT were morphologically normal (Supplementary Fig. S8a), whereas many *nup1* pollen grains were collapsed (Supplementary Fig. S8b, c). In addition, viable *nup1* pollen grains exhibited a thinner exine surface compared with WT (Supplementary Fig. S8d-k).

To distinguish lethal pollen in *nup1* mutant was due to gametophytic or sporophytic defect, we analyzed self progenies of NUP1 heterozygous plant (A/a). Among 229 descendants, 56 plants (about 24.5%) displayed sterile phenotype (aa). In addition, we crossed *nup1-4* with *quartet1* (*qrt1*) mutant (Preuss et al. 1994). In *qrt1* plants, the four products of a single meiosis are attached together throughout pollen development (Supplementary Fig. S9a). The *nup1*/*NUP1 qrt1* plant produced four normal attached mature pollen grains (Supplementary Fig. S9b). However, zero to four shriveled pollen grains were detected in tetrads from *nup1qrt1* mutant (Supplementary Fig. S9c-g). These results indicate that sporophytic defect give rise to aborted pollen grains in *nup1* mutant.

nup1 mutants produce large pollen grains

We also observed that *nup1* mutants produced large pollen grains (Fig. 6a, c; Supplementary Fig. S10a, c). The average diameter of WT pollen grains was approximately 21 μm, whereas the average diameter of *nup1* pollen grains was approximately 25 μm (Fig. 6b, d; Supplementary Fig. S10b, d). Since cell size is usually correlated with endoreduplication (Barow 2006; Lee et al. 2009), we performed flow cytometry analysis to see if the large pollen grain phenotype of *nup1* was accompanied by increased endoreduplication. Indeed, *nup1* pollen had a higher ploidy level compared with that of the WT (Fig. 6e; Supplementary Fig. S10e).

Pollen development in *nup1* is arrested during mitosis I

To determine at which developmental stage *nup1* pollen was abnormal, we performed transverse sections of *nup1* anthers at various developmental stages. Pollen from *nup1* anthers appeared normal during the tetrad and microspore stages (Fig. 7a). However, by the early bicellular stage, some *nup1* pollen grains were obviously smaller and exhibited collapsed cytosol (Fig. 7a). At later stages, shriveled pollen grains were observed (Fig. 7a).

We further stained *nup1* and WT pollen grains with DAPI to visualize the number and position of nuclei. At the microspore stage, there was no difference between *nup1* and WT pollen grains (Fig. 7b). However, at the bicellular stage, some *nup1* mutant pollen grains exhibited no DAPI staining (Fig. 7b). The number of unstained *nup1* pollen grains increased at tricellular stage (Fig. 7b).

Together, these results indicate that *nup1* pollen grains were arrested during the first mitosis process.

Reproduction-related genes are downregulated in *nup1* mutants

To gain insight into the molecular mechanism by which NUP1 affects male and female gametogenesis, we performed transcriptome analysis using RNA-sEq. We found that 134 genes were upregulated and 689 genes were downregulated in *nup1*, respectively [fold change > 2 and false discovery rate (FDR) < 0.01] (Fig. 8a; Supplementary Dataset 1). Consistent with the observed phenotypes, GO analysis of the downregulated genes showed a significant enrichment for genes involved in pollination, reproductive developmental process, cell differentiation, and regulation of cell size (ranked by FDR < 0.01) (Fig. 8b; Supplementary Dataset 2; Supplementary Fig. S11). Whereas top recurring GO terms

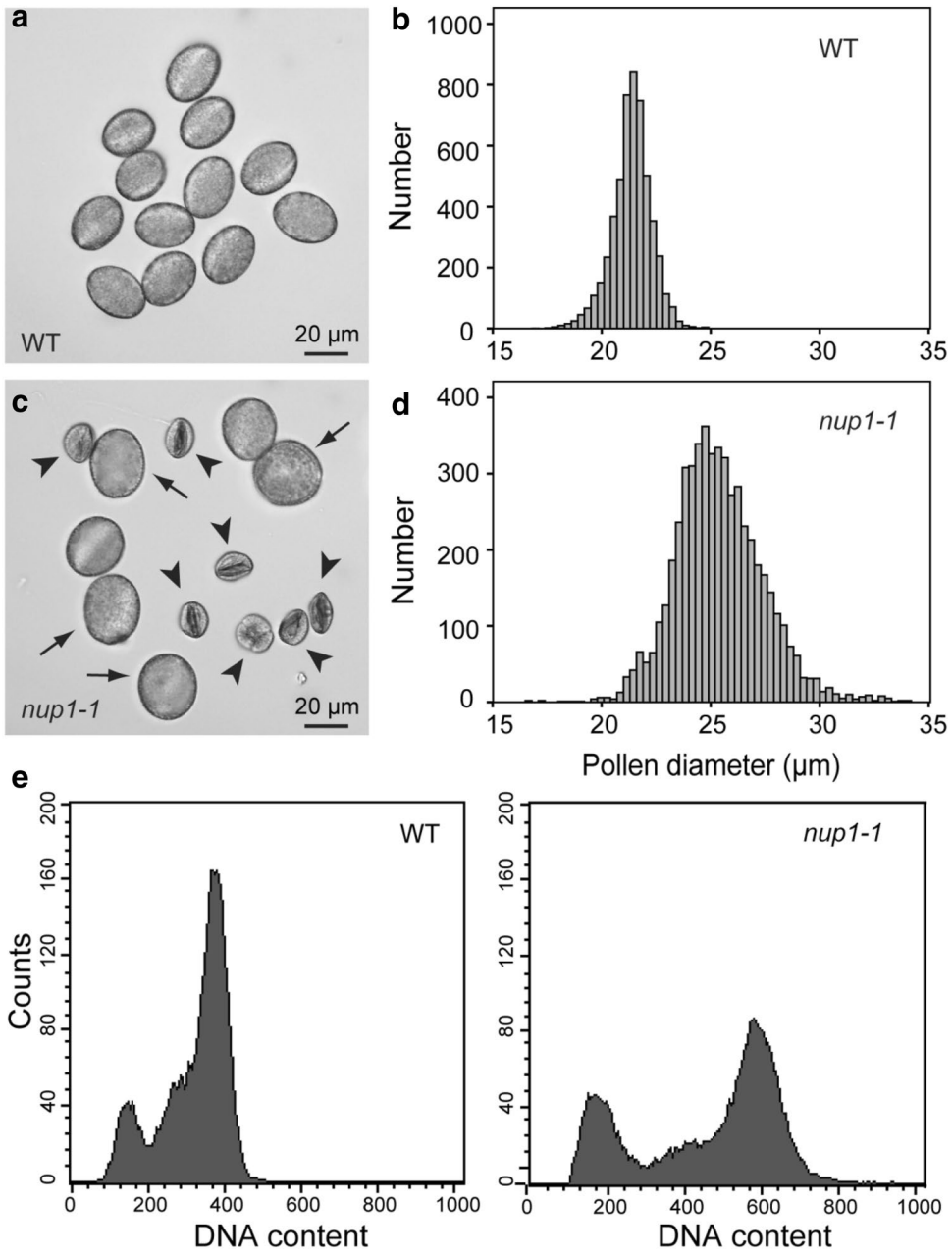

Fig. 6 *nup1* mutants produce large pollen grains with increased DNA content. **a, c** Mature pollen grains from WT (**a**) and *nup1-1* plants (**c**). Arrowheads indicate large pollen grains; arrows indicate aborted pollen grains. **b, d** Pollen grain size distribution of WT (**b**) and *nup1-1* (**d**). $n = 5203$ for WT and 5222 for *nup1-1*. **e** DNA content in pollen grains of WT and *nup1* mutant. Mature pollen grains from 13-stage flowers of WT and *nup1-1* mutant were collected, and DNA content was determined by flow cytometry. Approximately 20,000 pollen grains were analyzed for each genotype

among the upregulated genes were related to response to stimulus and cell death (Supplementary Fig. S12). Given that mitosis of male and female gametophyte was affected in *nup1* mutant, we identified many genes involved in mitotic process in our RNA-seq data (Supplementary Dataset 3). For validation, the transcript levels of 19 reproduction-related genes were analyzed by qRT-PCR. The qRT-PCR results were consistent with the RNA-seq results (Fig. 8c). Altogether, these data suggest that the gametogenesis defects observed in *nup1* mutants are caused by downregulation of reproduction-related genes.

Discussion

In this study, we analyzed the fertility defects of *nup1* mutant. We found that both male and female gametogenesis were aberrant in *nup1* mutant. *nup1* female gametophytes were arrested during meiosis; its male gametophytes were arrested during mitosis I. The developmental defect in *nup1* gametophytes was accompanied by reduced expression of reproduction-related genes. These results suggest that NUP1 plays a role in gametogenesis.

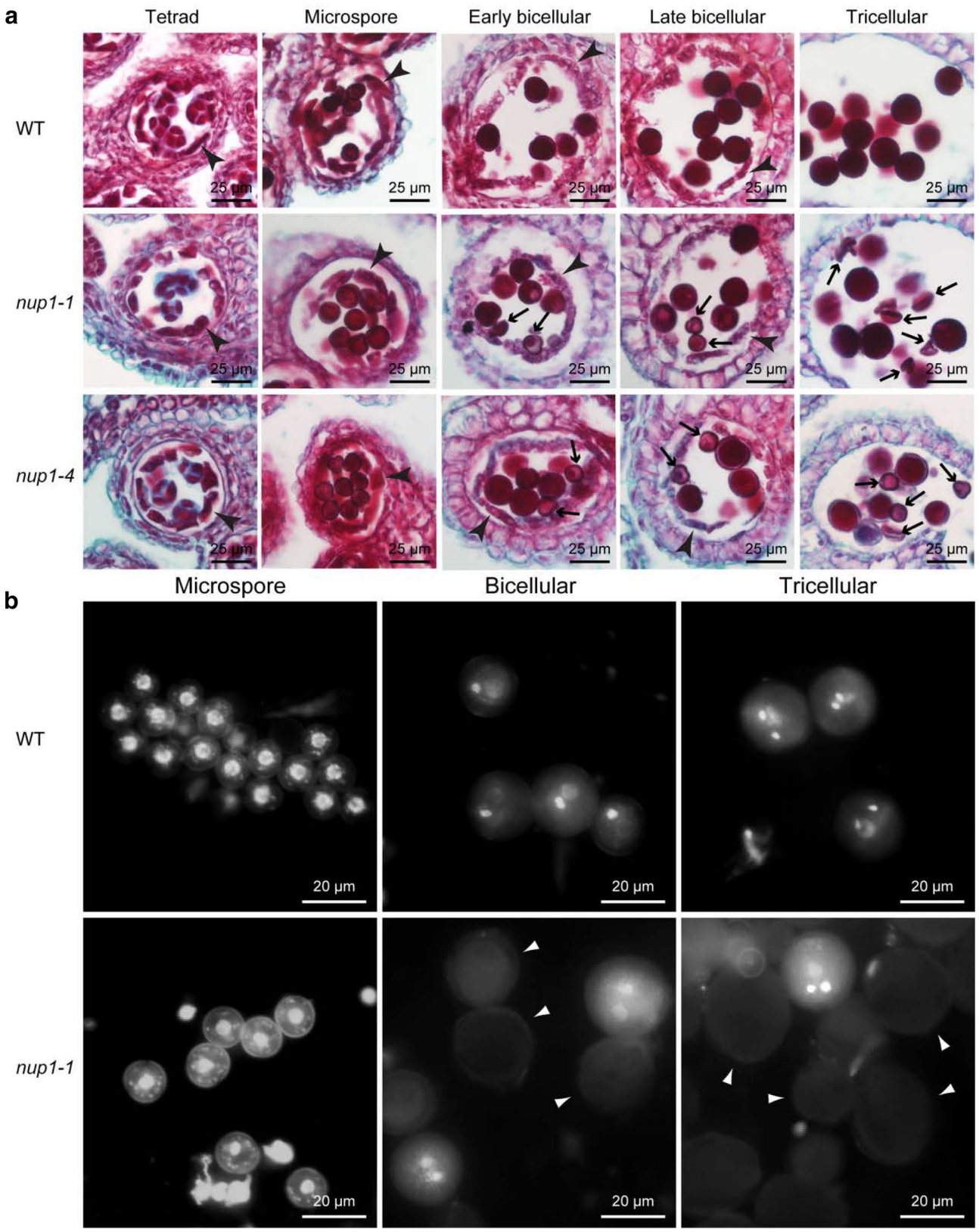
a
Tetrad
Microspore
Early bicellular
Late bicellular
Tricellular
WT
nup1-1
nup1-4
25 μm
b
Microspore
Bicellular
Tricellular
WT
nup1-1
20 μm

◂**Fig. 7** *nup1* pollen grains were arrested at mitosis I. **a** Parafin sections of WT and *nup1* anthers at different developmental stages. Aborted pollen grains (indicated by black arrows) were observed in *nup1*anthers at the early bicellular stage. Arrowheads indicate the tapetum. **b** DAPI staining of WT and *nup1* pollens at different developmental stages. Pollen grains from *nup1-1* and WT anthers were stained with DAPI to label nuclei and visualized with fluorescent microscope. Nonstaining pollen grains (indicated by arrows) were first observed at the bicellular stage

NUP1 affects meiosis of MMC

NUPs are components of NPC, which mediates transport of RNAs and proteins between the nucleus and cytoplasm (Xu and Meier 2008; Meier and Brkljacic 2009). Mutants of *NUP* genes share some common phenotypes such as retarded growth, early flowering, blocked mRNA export, and altered nuclear morphology (Tamura et al. 2010; Lu et al. 2010; Tamura and Hara-Nishimura 2011; Parry 2014; Du et al. 2016). However, more evidences indicate that individual NUPs play specific cellular roles and influence plant growth and development by different molecular mechanisms. For example, NUP98 regulates the shade avoidance response in Arabidopsis by activating shade-induced gene expression (Gallemí et al. 2016). NUP88/MOS7 was demonstrated to be required for spindle assembly and cell plate formation during gametophyte mitosis (Park et al. 2014). Here we show for the first time that NUP1 is required for the meiosis of MMC. More than half of *nup1* female gametophytes could

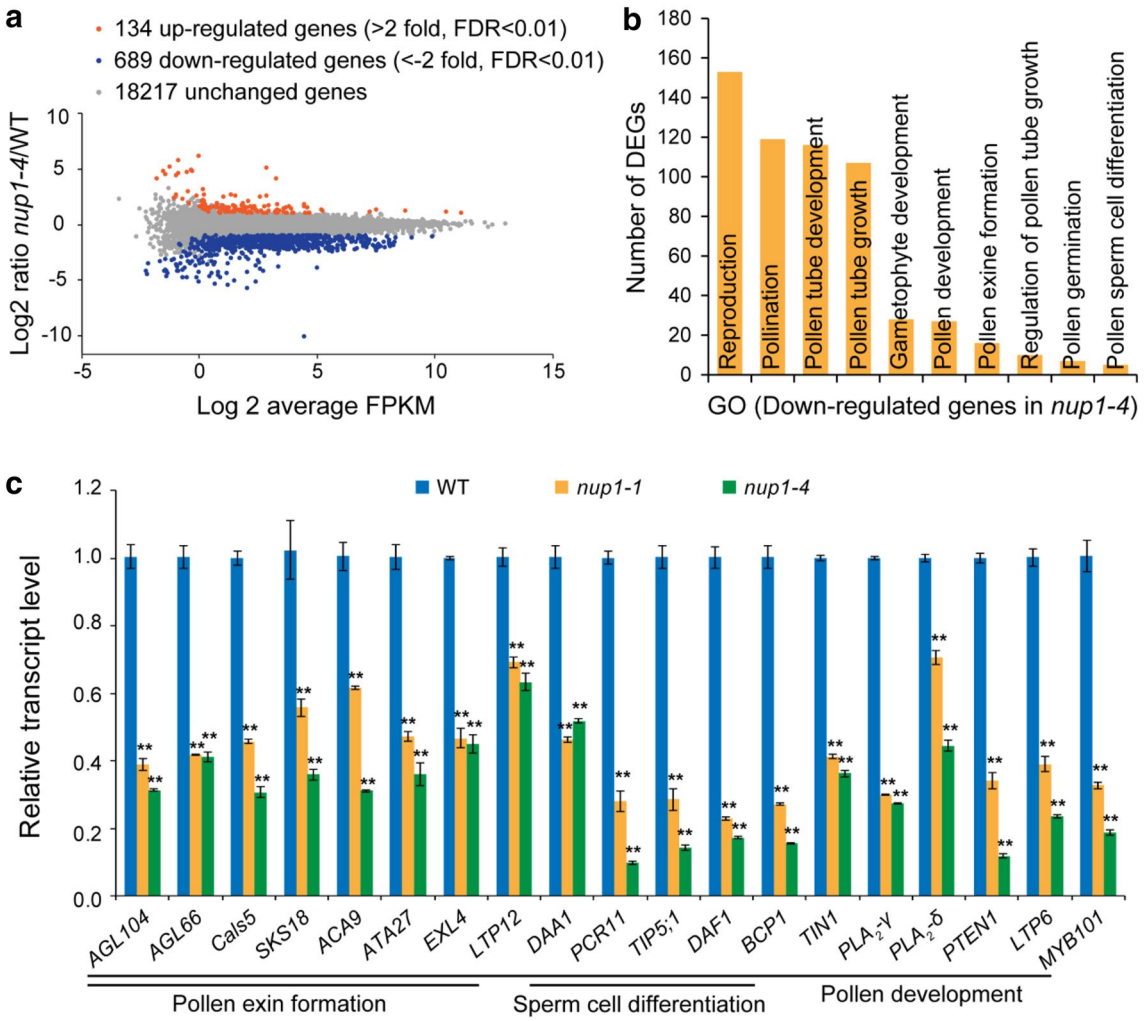

Fig. 8 *NUP1* mutation causes downregulation of genes involved in reproduction. **a** RNA-seq scatter plot showing differentially transcribed genes in WT and *nup1-4*. FDR, false discovery rate; FPKM, fragments per kilobase of transcript per million fragments mapped. **b** GO analysis of the downregulated genes in *nup1-4*. GO functional enrichment was analyzed using the online tool AgriGO (http://bioinfo.cau.edu.cn/agriGO/index.php). **c** qRT-PCR analysis of downregulated genes involved in pollen development. Expression levels relative to *TIP41* are displayed. Similar results were obtained from three independent experiments. Shown are results from one experiment. Error bars indicate the standard deviation (SD). $^{**}P < 0.01$ by Student's *t* test

not develop to stage FG1 (Tables 2, 3; Fig. 4; Supplementary Fig. S6), with some ovules arrested prior to meiosis (Fig. 4d, e), some ovules arrested after meiosis I (Fig. 4f; Supplementary Fig. S6), and some aborted just after meiosis II (Fig. 4g, h). In addition, our results indicated that formed position of cell plate was affected during meiosis of *nup1* ovules (Fig. 5). These results indicate that NUP1 influences the initiation, execution, exit, and cell plate formation during the meiosis of MMC. NUPs have been demonstrated to play important roles during meiosis in yeast and animals. In *Saccharomyces cerevisiae*, NUP2, NUP60 and NUP84 were found to have a meiotic function (Chu et al. 2017). A 125 aa region of NUP2 was necessary and sufficient for its meiotic role, therefore this region was called meiotic autonomous region (MAR) (Chu et al. 2017). NUP2-MAR was required for meiotic chromosome organization (Chu et al. 2017). In *Schizosaccharomyces pombe*, Nup132 regulates kinetochore assembly during meiotic prophase (Yang et al. 2015). The *C. elegans* nucleoporin MEL-28/ELYS interacts with PP1 (protein phosphatase 1) to mediate meiotic chromosome segregation (Hattersley et al. 2016). Nup107 is required for cytokinesis in *Drosophila* male meiosis (Hayashi et al. 2016). Whether the Arabidopsis NUP1 affects MMC meiosis through regulating chromosome organization or segregation requires further analysis.

NUP1 is required for mitosis of both male and female gametophytes

Mitosis of both male and female gametophytes of *nup1* mutants was defective. Male gametophytes of *nup1* were arrested at mitosis I (Fig. 7). Less than 17% of *nup1* female gametophytes could finish the three rounds of mitosis to form mature female gametes (Tables 2, 3). Therefore, ovules stayed at FG1, FG2-3, and FG4 were observed in mature pistils of *nup1* mutants (Table 2; Fig. 4i–k). These results indicate a mitotic function of the Arabidopsis NUP1. Mitotic functions have been reported for several NUPs including the Arabidopsis MOS7/NUP88 (Park et al. 2014), the vertebrate Nup98, Nup133, Nup188, and Nup153 (Lussi et al. 2010; Cross and Powers 2011; Bolhy et al. 2011; Itoh et al. 2013), the *C. elegans* NPP-10, NPP-13, and NPP-20 (Ferreira et al. 2017), and the yeast Nup1 (Harper et al. 2008). These NUPs participate in mitosis by affecting spindle assembly, kinetochore organization, and spindle checkpoint activity (Harper et al. 2008; Lussi et al. 2010; Cross and Powers 2011; Bolhy et al. 2011; Itoh et al. 2013; Ferreira et al. 2017). Nup153 interacts with the spindle assembly checkpoint protein Mad1 and affects its phosphorylation status (Lussi et al. 2010). The Arabidopsis NUP1 is an ortholog of the yeast NUP1 and animal NUP153 (Neumann et al. 2006; Lu et al. 2010). The Arabidopsis NUP1 is highly dynamic on the nuclear envelope, suggesting a dynamic interaction with other proteins (Tamura et al. 2010). Future work is required to determine whether the Arabidopsis NUP1 interact with the microtubule or the spindle assembly checkpoint proteins.

NUP1 deficiency reduces expression level of reproduction-related genes

Increasing evidence has pointed to a transport-independent role for the NUPs in regulating gene expression. NPC provides a platform for regulating gene transcription by anchoring genes, recruiting transcription factors, or post-transcriptional modification (Dieppois and Stutz 2010). A recent research found that Nup62, Nup93 and Nup155 form a negative regulatory loop to control the chromatin tethering state in *Drosophila* male germline and somatic cells (Breuer and Ohkura 2015). In plants, NUPs have also been reported to regulate gene expression through tethering of certain genes (Smith et al. 2015; Gallemí et al. 2016). In mouse embryonic stem cells, Nup153 recruits the polycomb-repressive complex 1 (PRC1) to a subset of developmental genes to inhibit their expression to maintain the pluripotency of the stem cells (Jacinto et al. 2015). Nup98 interacts with the 3′-UTR of p21 (a target gene of the p53 tumor suppressor) mRNA to protect it from degradation by the exosome (Singer et al. 2012). Nup106, Nup120, and Rae1 selectively destabilize meiotic mRNAs in vegetative fission yeast (Sugiyama et al. 2013). Our transcriptome analysis results showed that expression levels of reproduction-related genes were reduced dramatically in the Arabidopsis *nup1* mutant (Fig. 8; Supplementary Fig. S11, S12 and supplementary dataset). This finding implicates that NUP1 may regulate expression level of reproduction-related genes. Similar to those NUPs that can regulate gene expression, NUP1 is a peripheral NUP of the NPC and is highly mobile (Tamura et al. 2010; Lu et al. 2010). Further experiments are required to determine whether NUP1 can directly regulate gene transcription.

Author contribution statement SM conceived the project and designed experiments. SB performed most of the experiments; GS and ZL helped with parafin sections; GL, MA, and QW helped with cloning and genotyping. SM analyzed the data and wrote the article.

Acknowledgements We thank The Nottingham Arabidopsis Stock Center (NASC) for the T-DNA insertions, John Innes Centre for the pGREENII0229 vector. We thank Ruming Liu and Yajuan Wan for technical assistance in the use of confocal and cell cytometry equipment, respectively. This work was supported by grants from the National Science Foundation of China (31570247, 91417308, and 31460453); the Natural Science Foundation of Tianjin (no. 14JCYBJC41200).

Funding This work was supported by grants from the National Natural Science Foundation of China (31570247, 91417308, and 31460453).

Compliance with ethical standards

Conflict of interest The authors declare that they have no conflict of interest.

References

Alexander MP (1969) Differential staining of aborted and nonaborted pollen. Stain Technol 44:117–122

Allen JL, Douglas MG (1989) Organization of the nuclear pore complex in *Saccharomyces cerevisiae*. J Ultra Mol Struct Res 102:95–108

Barow M (2006) Endopolyploidy in seed plants. Bioessays 28:271–281

Boeglin M, Fuglsang AT, Luu DT et al (2016) Reduced expression of *AtNUP62* nucleoporin gene affects auxin response in *Arabidopsis*. BMC Plant Biol 16:2

Bolhy S, Bouhlel I, Dultz E et al (2011) A Nup133-dependent NPC-anchored network tethers centrosomes to the nuclear envelope in prophase. J Cell Biol 192:855–871

Breuer M, Ohkura H (2015) A negative loop within the nuclear pore complex controls global chromatin organization. Genes Dev 29:1789–1794

Cheng YT, Germain H, wiermer M et al (2009) Nuclear pore complex component MOS7/Nup88 is required for innate immunity and nuclear accumulation of defense regulators in Arabidopsis. Plant Cell 21:2503–2516

Chu DB, Gromova T, Newman TAC, Burgess SM (2017) The nucleoporin Nup2 contains a meiotic-autonomous region that promotes the dynamic chromosome events of meiosis. Genetics 206:1319–1337

Clough SJ, Bent AF (1998) Floral dip: a simplified method for Agrobacterium-mediated transformation of *Arabidopsis thaliana*. Plant J 16:735–743

Cross MK, Powers MA (2011) Nup98 regulates bipolar spindle assembly through association with microtubules and opposition of MCAK. Mol Biol Cell 22:661–672

Dieppois G, Stutz F (2010) Connecting the transcription site to the nuclear pore: a multi-tether process that regulates gene expression. J Cell Sci 123:1989–1999

Dong CH, Hu X, Tang W et al (2006) A putative *Arabidopsis* nucleoporin, AtNUP160, is critical for RNA export and required for plant tolerance to cold stress. Mol Cell Biol 26:9533–9543

Du Z, Zhou X, Ling Y et al (2010) agriGO: a GO analysis toolkit for the agricultural community. Nucleic Acids Res 38:W64–W70

Du J, Gao Y, Zhan Y et al (2016) Nucleocytoplasmic trafficking is essential for BAK1- and BKK1-mediated cell-death control. Plant J 85:520–531

Ferreira J, Stear JH, Saumweber H (2017) Nucleoporin NPP-10, NPP-13 and NPP-20 are required for HCP-4 nuclear import to establish correct centromere assembly. J Cell Sci 130:963–974

Fiserova J, Kiseleva E, Goldberg MW (2009) Nuclear envelope and nuclear pore complex structure and organization in tobacco BY-2 cells. Plant J 59:243–255

Galbraith DW, Harkins KR, Maddox JM et al (1983) Rapid flow cytometric analysis of the cell cycle in intact plant tissues. Science 220:512–527

Gallemí M, Galstyan A, Paulišić S et al (2016) DRACULA2 is a dynamic nucleoporin with a role in regulating the shade avoidance syndrome in Arabidopsis. Development 143:1623–1631

Genenncher B, Wirthmueller L, Roth C et al (2016) Nucleoporin-regulated MAP kinase signaling in immunity to a necrotrophic fungal pathogen. Plant Physiol 172:1293–1305

Goldberg MW, Allen TD (1996) The nuclear pore complex and lamina: Three-dimensional structures and interactions determined by field emission in-lens scanning electron microscopy. J Mol Biol 257:848–865

Gu Y, Zebell SG, Liang Z et al (2016) Nuclear pore permeabilization is convergent signaling event in effector-triggered immunity. Cell 166:1526–1538

Harper NC, Al-Greene NT, Basrai MA, Belanger KD (2008) Mutations affecting spindle pole body and mitotic exit network function are synthetically lethal with a deletion of the nucleoporin *NUP1* in *S. cerevisiae*. Curr Genet 53:95–105

Hattersley N, Cheerambathur D, Moyle M et al (2016) A nucleoporin docks protein phosphatase 1 to direct meiotic chromosome segregation and nuclear assembly. Dev Cell 38:463–477

Hayashi D, Tanabe K, Katsube H, Inoue YH (2016) B-type nuclear lamin and the nuclear pore complex Nup107-160 influences maintenance of the spindle envelope required for cytokinesis in *Drosophila* male meiosis. Biol Open 5:1011–1021

Itoh G, Sugino S, Ikeda M et al (2013) Nucleoporin Nup188 is required for chromosome alignment in mitosis. Cancer Sci 104:871–879

Jacinto FV, Benner C, Hetzer MW (2015) The nucleoporin Nup153 regulates embryonic stem cell pluripotency through gene silencing. Genes Dev 29:1224–1238

Johnson-Brousseau SA, McCormick S (2004) A compendium of methods useful for characterizing Arabidopsis pollen mutants and gametophytically-expressed genes. Plant J 39:761–775

Kim D, Pertea G, Trapnell C et al (2013) TopHat2: accurate alignment of transcriptomes in the presence of insertions, deletions and gene fusions. Genome Biol 14:R36

Lee HO, Davidson JM, Duronio RJ (2009) Endoreplication: polyploidy with purpose. Genes Dev 23:2461–2477

Lu Q, Tang X, Tian G et al (2010) Arabidopsis homolog of the yeast TREX-2 mRNA export complex: components and anchoring nucleoporin. Plant J 61:259–270

Lussi YC, Shumaker DK, Shimi T, Fahrenkrog B (2010) The nucloporin Nup153 affects spindle checkpoint activity due to an association with MadI. Nucleus 1:71–84

Meier I, Brkljacic J (2009) The nuclear pore and plant development. Curr Opin Plant Biol 12:87–95

Men S, Boutté Y, Ikeda Y et al (2008) Sterol-dependent endocytosis mediates post-cytokinetic acquisition of PIN2 auxin efflux carrier polarity. Nat Cell Biol 10:237–244

Neumann N, Jeffares DC, Poole AM (2006) Outsourcing the nucleus: nuclear pore complex genes are no longer encoded in nucleomorph genomes. Evol Bioinform 2:23–34

Park GT, Frost JM, Park JS et al (2014) Nucleoporin MOS7/Nup88 is required for mitosis in gametogenesis and seed development in Arabidopsis. Proc Natl Acad Sci USA 111:18393–18398

Parry G (2014) Components of the *Arabidopsis* nuclear pore complex play multiple diverse roles in control of plant growth. J Exp Bot 65:6057–6067

Parry G, Ward S, Cernac A et al (2006) The *Arabidopsis* SUPPRESSOR OF AUXIN RESISTANCE proteins are nucleoporins with an important role in hormone signaling and development. Plant Cell 18:1590–1603

Preuss D, Rhee SY, Davis RW (1994) Tetrad analysis possible in Arabidopsis with mutation of the *QUARTET* (*QRT*) genes. Science 264:1458–1460

Roberts K, Northcote DH (1970) Structure of the nuclear pore in higher plants. Nature 228:385–386

Singer S, Zhao R, Barsotti AM et al (2012) Nuclear pore component Nup98 is a potential tumor suppressor and regulates post-transcriptional expression of select p53 target genes. Mol Cell 48:799–810

Smith S, Galinha C, Desset S et al (2015) Marker gene tethering by nucleoporins affects gene expression in plants. Nucleus 6:471–478

Sugiyama T, Wanatabe N, Kitahata E et al (2013) Red5 and three nuclear pore components are essential for efficient suppression of specific mRNAs during vegetative growth of fission yeast. Nucleic Acids Res 41:6674–6686

Tamura K, Hara-Nishimura I (2011) Involvement of the nuclear pore complex in morphology of the plant nucleus. Nucleus 2:168–172

Tamura K, Fukao Y, Iwamoto M et al (2010) Identification and characterization of nuclear pore complex components in *Arabidopsis thaliana*. Plant Cell 22:4084–4097

Tamura K, Fukao Y, Hatsugai N et al (2017) Nup82 functions redundantly with Nup136 in a salicylic acid-dependent defense response of *Arabidopsis thaliana*. Nucleus 8:301–311

Trapnell C, Roberts A, Goff L et al (2012) Differential gene and transcript expression analysis of RNA-seq experiments with TopHat and Cufflinks. Nat Protoc 7:562–578

Walde S, Kehlenbach RH (2010) The Part and the Whole: functions of nucleoporins in nucleocytoplasmic transport. Trends Cell Biol 20:461–469

Wiermer M, Cheng YT, Imkampe J et al (2012) Putative members of the Arabidopsis Nup107-160 nuclear pore sub-complex contribute to pathogen defense. Plant J 70:796–808

Xu XM, Meier I (2008) The nuclear pore comes to the fore. Trends Plant Sci 13:20–27

Yang HJ, Asakawa H, Haraguchi T, Hiraoka Y (2015) Nup132 modulates meiotic spindle attachment in fission yeast by regulating kinetochore assemble. J Cell Biol 211:295–308

Yang Y, Wang W, Chu Z et al (2017) Roles of nuclear pores and nucleo-cytoplasmic trafficking in plant stress responses. Front Plant Sci 8:574

Zhang Y, Li X (2005) A putative nucleoporin 96 is required for both basal defense and constitutive resistance responses mediated by *suppressor of npr1-1, constitutive 1*. Plant Cell 17:1306–1316

Zhang X, Sun S, Nie X et al (2016) Sterol methyl oxidases affect embryo development via auxin-associated mechanisms. Plant Physiol 171:468–482